AAS 01-223

MITIGATION OF THE EFFECTS OF ECLIPSE BOUNDARY CROSSINGS ON THE NUMERICAL INTEGRATION OF ORBIT TRAJECTORIES USING AN ENCKE TYPE CORRECTION ALGORITHM

James Woodburn†

The proper application of a shadow model during the integration of orbit trajectories requires that the solar radiation pressure be sampled adequately during transitions between lighting conditions. An integration scheme is presented in which the lighting condition is held constant across steps of a primary integrator. If the lighting condition changes during that step, then an Encke-like integration is performed to correct the state at the end of the primary integration step. The effectiveness of this technique is presented for a set of Low Earth Orbits utilizing various combinations of the equations of motion and numerical integration methods.

INTRODUCTION

The computation of orbit trajectories using special perturbations techniques has advantages of being conceptually simple and capable of producing accurate results. The basic concept is to compute the sum of all accelerations acting on the satellite at a given point in time and apply a numerical integration procedure to transition the state of the satellite into the future. It is typically convenient to view the numerical integration procedures as "black boxes" where we adhere to specific input and output interfaces and blindly trust the process inside. In some cases, however, it is necessary to consider the assumptions used in the derivation of the numerical integration procedures to determine if the problem to be solved complies with these assumptions.

One area where the assumptions of the numerical integration procedure are often violated is in the modeling of effects of solar radiation pressure (SRP). When the acceleration due to solar radiation pressure is included in the force model, it is necessary to account for the occultation of the Sun by the Earth and/or other large bodies. The most common models for the shadow of the Earth and other planetary bodies are the conical model and the dual cone model. Each of these models has hard boundaries across which the acceleration due to SRP changes in form. These changes result in a discontinuity in the second order derivative of the position in the case of a cylindrical model and in a

† Chief Orbital Scientist, Analytical Graphics, Inc., Senior Member, AIAA

discontinuity or near discontinuity in the third derivative of the position in the case of a dual cone model. The existence of these discontinuities due to the shadow models violates the assumption, made in the formulation of many numerical integration methods, that the accelerations are smooth and continuous.

The actual change in solar radiation pressure is not as sudden as that predicted by these models. Absorption and refraction of solar radiation by the atmosphere and the apparent deformation of the solar disk as seen through the Earth's atmosphere influence the level of illumination[1]. While detailed models of these phenomena exist, the complexity and computational burden imposed by such sophisticated shadow models has inhibited their widespread application[2]. In light of the fact that the common shadow models are not exact, the interaction of the model with the integration procedure may not be immediately assumed to affect the accuracy of trajectory computation. This interaction will, however, affect comparisons between orbit propagators and for that reason is worthy of study[3,4].

The effect of discontinuities in the simpler shadow models on the accuracy of the integrated trajectory, relative to a trajectory where the shadow model has been properly applied, is dependent upon how the integration method a steps across the boundary[2,5,6]. While the dual cone model predicts a smoother transition between lighting conditions than the cylindrical model, it not uncommon for a single integration step to span the penumbra period thus causing the change in acceleration to seem instantaneous. A recent study has shown that larger step sizes in the numerical integration process lead to larger errors being introduced into the trajectory[5]. This trend is in direct opposition to the typical desire to take the largest possible step sizes during orbit integration to reduce the computation time. Errors, in this context, are differences measured relative to the proper application of the shadow model.

In order to enable the use of larger steps during numerical integration while maintaining accuracy, a strategy is sought to mitigate the effects of the shadow boundary crossings. Lundberg *et al.* have devised an algorithm for correcting the errors resulting from the crossing of shadow boundaries for multi-step integrators[6]. This algorithm is an improvement of an algorithm originally devised by Hubbard and documented in the open literature by Anderle[7]. This algorithm allows for the preservation of the step size of the integrator, but is tightly coupled to the particular multi-step formulation. Lundberg also derived a method for determining the step size for a multi-step integrator using a fixed step size to minimize the errors due to crossing shadow boundaries[8]. The optimal step size is computed to avoid situations where the time between the closest integration node and the shadow remains fairly constant. In this situation, the numerical integration is in a form of resonance with the eclipsing of the satellite and the errors incurred during the crossings of the shadow boundaries are less likely to cancel out over time.

A new approach to the mitigation of shadow boundary crossing effects has been developed where the crossing of shadow boundaries is ignored in the main integration procedure. The crossings are detected at the end of the main integrator step and the state at the leading node of the integration process is corrected using the Encke method of orbit

integration. This technique allows for the preservation of the integration step size and is applicable to both single step and multi-step integration procedures.

SHADOW MODELS

The effects of crossing the shadow boundaries of two shadow models were investigated in a prior study. The cylindrical model, illustrated in Figure 1, assumes that the Sun is infinitely far away such that all light is coming from a direction parallel to the direction to the Sun. The shadow cast by the Earth may then be represented as a cylinder of infinite length. The acceleration due to solar radiation pressure is zero when the satellite is inside the cylinder. The particular implementation of the model used in this study does not assume the obstructing body to be spherical. The lighting condition is determined by detecting if the line from the satellite, parallel to the Sun direction, intersects the obstructing body, which allows for the use of an oblate shape for the Earth.

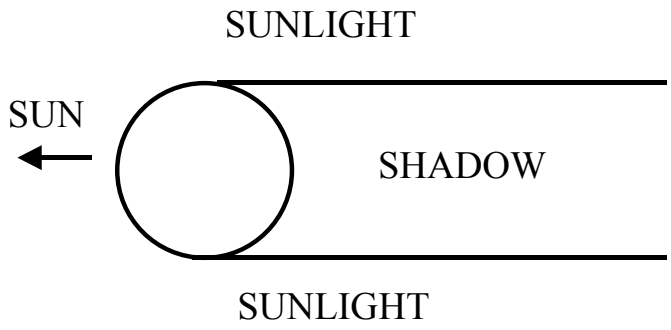

Figure 1. Cylindrical Shadow Model

The dual cone model accounts for the finite size and distance of the Sun, which establishes a region of partial illumination known as the penumbra region, shown in Figure 2. There are several common methods for computing the magnitude of the acceleration due to solar radiation pressure when the satellite is in the penumbra region. The method most consistent with the geometry of the model, and the one used in this study, is to scale the acceleration of the satellite if it were in direct sunlight by the fractional area of the visible solar disk. Other methods include (i) scaling the acceleration of the satellite if it were in direct sunlight based on a linear transition to full shadow and (ii) scaling the acceleration in full sunlight by one half. The shape of the obstructing body is not assumed to be spherical in the implementation of the dual cone model used for this study. The lighting condition is determined via comparison of the grazing angle of the line from the satellite to the apparent position of the Sun and the instantaneous half angle of the Sun. If the grazing angle is greater than the half angle, the satellite is in direct sunlight. If the grazing angle is smaller than the negative of the half angle, the satellite is in the umbra region. If the absolute value of the grazing angle is smaller than the half angle of the Sun, the satellite is in the penumbra region.

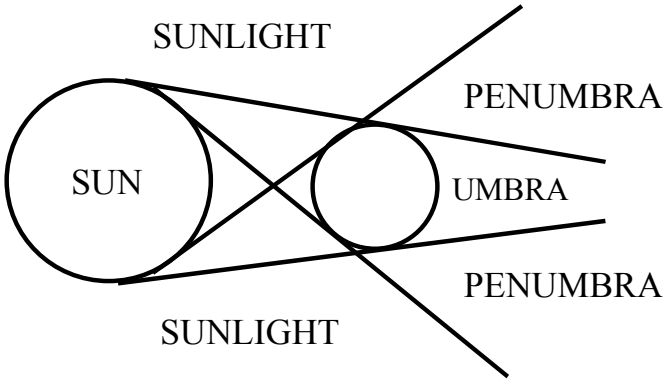

Figure 2. Dual Cone Shadow Model

FORMULATION

Since the errors introduced into the integration process are a result of rapid changes in the force model during an integration step, a reasonable approach to mitigating the effects of shadow boundary crossings is to stop the integration procedure at the shadow boundary. The integration process may then be restarted in the presence of the new set of accelerations. While simple in concept, this process is not computationally efficient. Restarting is especially costly for multi-step integration procedures, which require significant work to reinitialize.

Another approach is to maintain the shadow condition across each integration step and correct for modeling errors when necessary. This is the basis of the methods used by Hubbard and subsequently Lundberg, who derived analytical expressions for these corrections[6]. Hubbard provided corrections for SRP effect on the state assuming a cylindrical shadow model and based on an assumption of a constant acceleration due to SRP during the integration step. Lundberg extended Hubbard's method for application to a conical shadow model and included the effect of differential two-body accelerations. Both Hubbard and Lundberg implemented their correction schemes in conjunction with multi-step integrators. Lundberg also introduced the use of the interpolator equation of the multi-step integrator to estimate the corrected state.

An alternative method for correcting the state at the end of the integration step is to compute an update to the predicted state using an Encke-type integration about the current trajectory. Using this technique, the difference from a known trajectory is computed by numerically integrating the difference in the accelerations. The differences in accelerations in this case are the change in the SRP and the differential two-body acceleration. Differences in other accelerations will be considered negligible based on the assumption that the correction to the state will be very small. The differential equation for the correction to the state at the leading node of the integration procedure is[9],

$$\Delta\ddot{\vec{r}} = \frac{\mu}{\rho^3}\left[\left(1-\frac{\rho^3}{r^3}\right)\vec{r} - \Delta\vec{r}\right] + \kappa\vec{a}_{SRP}, \tag{1}$$

where $\vec{r}$ is the corrected state, $\vec{\rho}$ is the uncorrected state and μ is the gravitational parameter. κ is scale factor of the acceleration due to solar radiation pressure $\vec{a}_{SRP}$ which is set to the following

$$\kappa = 1 \quad \text{Umbra to Sunlight},$$
$$\kappa = -1 \quad \text{Sunlight to Umbra},$$
$$-1 < \kappa < 1 \quad \text{Penumbra}$$

and the state correction $\Delta\vec{r}$ is defined as

$$\Delta\vec{r} = \vec{r} - \vec{\rho}. \tag{2}$$

The initial conditions for the Encke integration are

$$\Delta\vec{r}_0 = 0, \tag{3}$$
$$\Delta\dot{\vec{r}}_0 = 0 \tag{4}$$

where the start time of the correction algorithm is the first time during the step when the actual lighting condition is different than the lighting condition used in the main integration procedure. This condition occurs due to the fact that the lighting condition is held constant across steps of the main integration procedure. The correction is computed by numerically integrating Eq. (1) from the correction start time until the end of the current step in the main integration procedure. The first term in Eq.(1) is the difference in the two body accelerations between the corrected and uncorrected trajectories and the second term accounts for the improper modeling of the acceleration due to SRP during the main integration step.

An array of recently computed ephemeris is maintained during the main integration process for use in the computation of the shadow boundary crossing times. These times are determined via an iterative procedure using interpolation of the stored array of ephemeris. The iterative procedure is terminated based on convergence to one millisecond for the cylindrical shadow model and 10 milliseconds for the dual cone shadow model. A tighter convergence criterion was placed on the cylindrical model since the change in the acceleration due to SRP is more sudden during the crossing of the shadow boundary. The interpolation method used in this study is 7^{th} order Lagrangian interpolation. Points along the reference trajectory for the Encke algorithm are also computed based on interpolation of the stored ephemeris. While interpolation will not produce the same level of fidelity as the numerical integration procedure, the correction algorithm is not particularly sensitive to the interpolated values. The overall effectiveness of the correction algorithm is not, therefore, adversely affected by the use of interpolation.

Each step of the correction procedure is restricted to a single lighting condition. When a cylindrical shadow model is used, a single correction step is taken. When a dual cone

shadow model is used, one or two correction steps may be required. The number of steps required to compute the correction depends on the number of shadow boundaries crossed. It is also important to note that the main integration procedure is configured to treat the penumbra condition the same as the umbra condition, setting the acceleration due to SRP to zero. This treatment of the penumbra condition in the main integration procedure results in the need to apply the correction procedure over the entire step for any step of the main integration procedure starting in the penumbra condition. The correction steps used in conjunction with the dual cone shadow model, based on the lighting conditions at the start and end of the main integration step, are given in Table 1. When two correction steps are required, the correction computed during the first step is used as the initial conditions to the second correction step.

TABLE 1. CORRECTION ALGORITHM FOR DUAL CONE SHADOW MODEL

Start Condition	End Condition	Correction Step 1	Correction Step 2
Sunlight	Penumbra	S/P to EOS	None
Sunlight	Umbra	S/P to P/U	P/U to EOS
Umbra	Penumbra	U/P to EOS	None
Umbra	Sunlight	U/P to P/S	P/S to EOS
Penumbra	Sunlight	SOS to P/S	P/S to EOS
Penumbra	Umbra	SOS to P/U	P/U to EOS
Penumbra	Penumbra	SOS to EOS	None

S/P, P/S – boundary between sunlight and penumbra

P/U, U/P – boundary between penumbra and umbra

SOS – start of main integration step, EOS – end of main integration step

IMPLEMENTATION

The correction algorithm has been implemented in conjunction with both single step and multi-step integration procedures. The single step procedures considered herein are the Runge-Kutta-Fehlberg 7-8 and the Bulirsch-Stoer[10,11]. The multi-step procedure is the 12th order Gauss-Jackson integrator using a Stormer predictor and a Cowell corrector[9,12]. Application of the correction algorithm with the single step procedures is fairly straightforward. The Encke correction is computed at the end of integration steps over which a change in the lighting condition has occurred. The correction is then added to the

current state at the leading node of the integration process and the main integration process is continued.

The process is significantly more complicated when a multi-step integrator is used. The additional complication results from the fact that the multi-step integrator uses acceleration data from prior steps to predict and correct estimates of the state at the next integration node. When the lighting condition changes during a particular step of the integrator, the set of accelerations for points going into the future are inconsistent with the stored accelerations at prior integration nodes. To account for this problem, the method of modified back differences is employed to add or subtract the SRP accelerations from the table of stored accelerations depending on whether the trajectory is entering or leaving the sunlit region of space. To illustrate the quantities in need of update, the Stormer prediction equation is presented as:

$$\vec{r}_{n+1}^{\,p} = h^2\left[\vec{S}_n^{II} + \sum_{i=0}^{j} C_i \ddot{\vec{r}}_{n-i}\right], \tag{5}$$

where h is the step size, $\vec{S}_n^{II}$ is the vector of second sums of the accelerations and C_i are coefficients specific to the order of the integration. To facilitate the addition or subtraction of accelerations due to SRP, the SRP accelerations are computed without a shadow model at each integration node and stored in parallel with the back acceleration table. The total acceleration at the current node must also be updated to account for the difference in the two-body acceleration, which results from the state correction[6]. Differences in other perturbing accelerations resulting from the update of the state at the leading node are assumed to be small and are not computed. Finally, the first and second sums must be reconstructed based upon the updated state at the leading node and the updated acceleration table. At this point the back acceleration table and sums include data that is consistent with the accelerations experienced during the forward integration process. The updated table is still not internally consistent, however, since the tabulated accelerations were computed at positions that would not be achieved by propagating backwards with the new accelerations. This issue is a potential subject for further study.

TEST CASES

A set of test cases for LEO orbits was run to determine the effectiveness of the correction algorithm. The initial conditions for the test cases are given in Table 2.

TABLE 2. INITIAL CONDITIONS

Epoch	a (km)	e	I (deg)	Ω (deg)	ω (deg)	ν (deg)	C_p	A/M (m^2/kg)	SC Step Size (sec)
1 Jun 2000 00:00:00	7000.0	0.0	55.0	220.0->280.0 steps of 5.0	0.0	90.0	2.0	0.02	30.0

The initial conditions in Table 2 are identical to those used in a previous study with the exception of the initial true anomaly[5]. The reason for the change in the initial true anomaly

is to avoid a change in lighting condition before a sufficient history of integrated points has been produced to support accurate interpolation. The test cases were run with both cylindrical and conical shadow models using the integration procedures listed in Table 3.

TABLE 3. INTEGRATION METHODS

Method	Order	ODE order	Type
Runge-Kutta-Fehlberg 7-8 (RK)	7	1st	Single step
Bulirsch-Stoer (BS)	N/A	1st	Single step
Stormer-Cowell (SC)	12	2nd	Multi-step

Table 4 contains reference data that was generated to provide a measure of the achievable accuracy of each combination of integration procedure and equations of motion. In Table 4, the abbreviation COW is used to indicate that the equations of motion were of the Cowell's formulation and the abbreviation VOP is used to indicate that the equations of motion were the variation of parameters formulation in universal variables as describe by Herrick[13]. Trajectories were generated for each set of initial conditions including the effects of SRP in the absence of a shadow model. The RK and BS integrators were allowed to vary the step size during the integration. The SC integrator was run with a fixed step size, which was selected to ensure accurate trajectories. The accuracy of the trajectories was determined via comparison with a set of trajectories integrated with the RK integrator at the fixed step size of five seconds. Any degradation of accuracy observed when shadow models are used can be considered to be a result of the interplay between the shadow model and the integrator.

TABLE 4. REFERENCE ACCURACY

Combination	Minimum Error (mm)	Maximum Error (mm)	Average Error (mm)
BS/COW	0.005	0.13	0.058
BS/VOP	0.017	0.066	0.038
RK/COW	0.17	0.19	0.18
RK/VOP	2.3	8.5	5.3
SC/COW	0.001	0.011	0.004

The information in Table 4 shows that the various combinations of integrators and force models are consistent to a level of less than one centimeter over a day. The level of agreement would be less than 0.2 millimeter without the RK/VOP formulation. This is indicative of a slight problem in the error control of the RK integrator when it is combined with the VOP formulation of the equations of motion. The errors encountered when the shadow models were included are shown in Table 5. In Table 5, the abbreviation CYL is used to indicate that a cylindrical shadow model was used and DC is used to indicate that a dual cone shadow model was used. It is also important to note that the quantities in Table 5 are expressed in meters while the quantities in Table 4 were expressed in millimeters.

TABLE 5. TRAJECTORY ERRORS WITH NO MITIGATION

Combination	Minimum Error (m)	Maximum Error (m)	Average Error (m)
BS/COW/CYL	0.15	2.0	0.84
BS/COW/DC	0.084	5.1	1.4
BS/VOP/CYL	0.53	1.7	0.62
BS/VOP/DC	0.15	1.9	0.78
RK/COW/CYL	0.044	1.6	0.52
RK/COW/DC	0.010	0.52	0.30
RK/VOP/CYL	0.26	3.2	1.4
RK/VOP/DC	0.18	2.3	1.1
SC/COW/CYL	0.18	1.4	0.54
SC/COW/DC	0.033	0.57	0.26

The same trajectories were computed using the Encke correction algorithm and the resulting trajectory errors are shown in Table 6. Note that the errors are expressed in millimeters as they were in Table 4. The results of Table 6 indicate the application of the correction algorithm removed almost all of the error introduced during the crossing of the shadow boundaries. The corrections appear to work equally well for Cowell and VOP formulations and for the cylindrical and dual cone shadow models. The largest errors are seen for the RK integration method paired with the VOP formulation of the equations of motion, but the error levels are not significantly different than those documented in the accuracy reference results of Table 4. This indicates that the majority of the error in the RK/VOP cases do not result from crossing shadow boundaries. The reference trajectories for the errors documented in Table 6 were generated using the RK/COW formulation with a five second step size. The integrator was also stopped on the shadow boundaries and

restarted during the computation of the reference trajectories. The process of stopping the integrator on the shadow boundary was subject to the same convergence limits as used in the Encke correction algorithm.

TABLE 6. TRAJECTORY ERRORS WITH MITIGATION

Combination	Minimum Error (mm)	Maximum Error (mm)	Average Error (mm)
BS/COW/CYL	0.19	1.7	1.0
BS/COW/DC	0.21	1.7	1.1
BS/VOP/CYL	0.12	1.7	0.98
BS/VOP/DC	0.17	1.7	1.0
RK/COW/CYL	0.13	0.15	0.14
RK/COW/DC	0.095	0.18	0.14
RK/VOP/CYL	3.4	9.1	5.7
RK/VOP/DC	3.5	8.8	5.4
SC/COW/CYL	1.6	2.4	2.0
SC/COW/DC	0.90	1.5	1.2

Statistics of the magnitude of the position and velocity corrections computed by the Encke correction algorithm were computed during the integration of the test cases for Table 6 and are presented in Table 7. The small magnitude of the observed corrections justifies the previous assumption that corrections to additional perturbing forces were not required during the update of the leading node accelerations for the multi-step integrator.

TABLE 7. MAGNITUDE OF ENCKE CORRECTIONS

	Minimum	Maximum	Average
Position	0.0 mm	7.9 mm	1.2 mm
Velocity	0.0 mm/s	0.053 mm/s	0.014 mm/s

CONCLUSIONS

A new approach to the mitigation of trajectory integration errors incurred during the crossing of shadow boundaries has been developed. The new approach holds the lighting condition constant across each step in the integration process. An Encke-type correction algorithm is then used to compensate for errors in the main integration process resulting from improper modeling of accelerations due to SRP. A study of a group of LEO trajectories has demonstrated the successful application of the mitigation procedure in conjunction with three different procedures for numerical integration including both single step and multi-step methods. The correction algorithm could be abstracted to provide corrections for other accelerations capable of experiencing sudden changes in form or magnitude.

REFERENCES

1. Vokrouhlicky, D., Farinella, P., Mignard, F., "Solar Radiation Pressure Perturbations for Earth Satellites I: A complete theory including penumbra transitions," *Astronomy and Astrophysics*, 1993.

2. Hujsak, R.S., "Solar Pressure," Proceedings of the Artificial Satellite Theory Workshop, USNO, 1993.

3. Chao, C.C., Warner, L.F., Cox, J., Thompson, R.C., Starchville, T.F., Cook, J.W., Woodburn, J. "IV&V of Three Astrodynamics Functions of the Satellite Tool Kit", Paper No. AIAA-2000-, AIAA/AAS Astrodynamics Conference, Denver, Colorado, August 2000.

4. SALAMA, A., NEMESURE, M., GUINN, J., BOLVIN, D., LEAVITT, R. "Compatibility of TOPEX/POSEIDON Trajectory Propagation with JPL and GSFC/FDF Operational Software", NASA Conference Publication 3265, Proceedings of the Flight Mechanics/Estimation Theory Symposium 1994, Goddard Space Flight Center, Greenbelt, Maryland, May 1994, pp. 169-178.

5. Woodburn, J. "Effects of eclipse boundary crossings on the numerical integration of orbit trajectories", Paper No. AIAA-2000-4027, AIAA/AAS Astrodynamics Conference, Denver, Colorado, August 2000.

6. Lundberg, J.B., Feulner, M.R., Abusali, P.A.M., Ho, C.S., "Improving the Numerical Integration Solution of Satellite Orbits in the Presence of Solar Radiation Pressure Using Modified Back Differences," AAS Paper 91-187, AAS/AIAA Space Flight Mechanics Meeting, Feb. 1991.

7. Anderle, R.J., "Geodetic Analysis Through Numerical Integration," Proceedings of the International Symposium on the Use of Artificial Satellites for Geodesy and Geodynamics, Athens, Greece, 1973.

8. Lundberg, J.B., "Mitigation of Satellite Orbit Errors Resulting from the Numerical Integration Across Shadow Boundaries," AAS Paper 95-408, Presented at the AAS/AIAA Astrodynamics Specialist Conference, Halifax, Nova Scotia, August 1995.

9. Vallado, David A., *Fundamentals of Astrodynamics and Applications*. New York: McGraw-Hill, 1997.

10. Fehlberg, E., "Some Old and New Runge-Kutta Formulas with Stepsize Control and Their Error Coefficients," *Computing*, Vol. 34, 1985, pp 265-270.

11. Stoer, J., Bulirsch, R., *Introduction to Numerical Analysis*. New York: Springer-Verlag, 1980.

12. Maury, J.L., Segal, G.P., "Cowell Type Numerical Integration as Applied to Satellite Orbit Computation," Goddard Space Flight Center, NASA Technical Report TM-X-63542, X-553-69-46.

13. Herrick, Samuel, *Astrodynamics Volume II.* London: Van Nostrand Reinhold Company, 1972